Order parameters in multisheet superconducting states

Z. Ye, H. Umezawa, and R. Teshima
The Theoretical Physics Institute, University of Alberta, Edmonton, Alberta, Canada T6G 2J1
(Received 26 June 1990; revised manuscript received 11 December 1990)

In this paper we study the multisheet superconducting system with intersheet and intrasheet pairing. In the mean-field approximation we derive and solve the coupled equations for the intersheet-pair and intrasheet-pair order parameters. We find that the order parameters are sensitive to both the intersheet and intrasheet coupling constants, however small or large the coupling constants may be. We define a characteristic parameter c which is a function of both coupling constants and is effectively useful in classifying the behavior of order parameters. To show a variety of temperature dependence, we present curves of order parameters versus temperature with different values of c. We see from these results that the intersheet pairs play a key role in maintaining the superconductivity. This suggests to us a significant aspect of lower-dimensional structure summarized by the term "pair multiplicity." We show also some exotic behavior of the specific heat. In cases of low-dimensional structure, the reliability of the mean-field approximation is in question. We analyze this question.

I. INTRODUCTION

An aim of this paper is to study superconducting states in a system of multiple two-dimensional sheets. There is considerable evidence that the high-T_c superconducting materials are highly anisotropic compounds.[1] This can be seen from its provskite structure. It is therefore natural to expect that this structure is, at least partly, responsible for the highly anisotropic behavior of these materials. Therefore, the research of the intrinsic properties of the layered material has attracted much attention. Study of the superconducting layered system today represents a classical problem.[2–4] Through this development we learned much about the proximity effect and tunneling effect between multilayers. The presence of the two-dimensional layer structure in high-T_c materials further encourages the research in this direction.

The most challenging question on high-T_c superconductivity is to ask what interaction makes T_c high and mediates the electron interaction. Many mechanisms have been proposed for high-T_c superconductivity,[5] but, whatever this interaction is, there is another question associated with intrinsic properties of two-dimensional sheets. It is well known that there cannot exist any superconducting state in an isolated two-dimensional sheet because the low dimensionality enhances the infrared effort of the quantum and thermal fluctuation of long-range correlation which quenches the superconducting orders (see, for example, Ref. 6). With this situation we have two possibilities. One is to make use of a kind of phase similar to the Kosterlitz-Thouless phase. There have been several papers which pursued this possibility. Another is to assume that the superconducting long-range correlation is created by electron tunneling or hopping through the multisheets. In this paper we take the second approach. Then, an interesting question is how this tunneling effect can overpower the destructive fluctuation effect mentioned above. There are two approaches to the multilayer system. The common one is to take advantage of knowledge on the proximity effect in a stack of thin-film layers. Considering a complex but realistic arrangement of layers in high-T_c materials, Tachiki *et al.*[7] recently presented a detailed theoretical analysis of multilayer superconductivity controlled by proximity effect. Another approach is to focus attention directly on the Cooper-pair tunneling interaction. We take this approach. To distinguish the two approaches, we conventionally use the word "sheet" for "layer." In the multisheet superconducting system, we have the bridge pair and in-sheet pair; the bridge pair is the Cooper pair with one electron in a sheet and its partner in the nearest sheet while the in-sheet pair is the Cooper pair of both electrons residing on the same sheet. Many experiments on high-T_c material have shown results different from those of the bulk BCS model. For example, it has been reported that the magnetic behavior of high-T_c material is anomalous.[8–10] To explain the anomalous temperature dependence of London penetration depths and low critical magnetic field, recently we presented a model of the multisheet superconducting states with bridge pairing only.[11] Our results agreed qualitatively with experiments. In our approach we do not ask what mediates the pair interaction, although an interesting candidate for this is the surface phonon associated with the sheets. Instead, we try to investigate the general features of multisheet superconducting systems. In the last paper we considered only the bridge pair. In this paper we extend our study to include *both* bridge and in-sheet pairs. We will concentrate on the study of the order parameters and specific heat, leaving the study of magnetic properties and mixed states to the future. We find that the temperature behavior of the order parameter for the system without in-sheet pairs (the system studied in the previous paper[11]) is different from that of the weak limit of in-sheet pair coupling. Furthermore, the weak limit of bridge pair interaction does not smoothly become the sit-

uation without the bridge pairs. This situation is more complicated than the one in Ref. 12. We will see that the results are quite sensitive to coupling strengths of both the bridge pairing and in-sheet pairing interactions. We introduce a particular parameter (denoted by c) consisting of these coupling constants which characterizes this sensitive behavior.

II. MODEL

We consider infinite sheets parallel to the a-b plane with spacing a. The sheet can move up and down along the c axis in order to absorb the recoil momentum of the electrons tunneling out. The coordinate system is chosen so that the a-b plane is the x-y plane and the z axis is along the c axis. The total Hamiltonian is

$$H = H_0 + H_{\rm int} , \tag{2.1}$$

where

$$H_0 = \sum_{i,\sigma} \psi_\sigma^\dagger(x,i)\varepsilon(-i\nabla)\psi_\sigma(x,i) \tag{2.2}$$

and

$$H_{\rm int} = (-\lambda_1)\sum_i \psi_\downarrow^\dagger(x,i)\psi_\uparrow^\dagger(x,i)\psi_\uparrow(x,i)\psi_\downarrow(x,i) + (-\lambda_2)\sum_i \tfrac{1}{2}[\psi_\downarrow^\dagger(x,i)\psi_\uparrow^\dagger(x,i+1)\psi_\uparrow(x,i+1)\psi_\downarrow(x,i) + \psi_\downarrow^\dagger(x,i)\psi_\uparrow^\dagger(x,i-1)\psi_\uparrow(x,i-1)\psi_\downarrow(x,i)] \tag{2.3}$$

with

$$\varepsilon(-i\nabla)e^{i\mathbf{k}\cdot\mathbf{x}} = \left[\frac{1}{2m}(k_x^2+k_y^2)-\mu_F\right]e^{i\mathbf{k}\cdot\mathbf{x}} . \tag{2.4}$$

Here $\psi_\sigma(x,i)$ is the electron Heisenberg field with spin σ on the ith sheet. The μ_F is the chemical potential. The first term in $H_{\rm int}$ is the pairing interaction among the electrons on the same sheet with the coupling λ_1 and the second term is the bridge pairing interaction with the coupling λ_2. Note here that the symbol x represents the two-dimensional vector $\mathbf{x}=(x,y)$ and the time t. In this model the electrons tunnel through sheets in pairs only. In Sec. IV B, we discuss the electromagnetic effects including the Coulomb potential effect.

In general, we have two order parameters:

$$\Delta_1(T) = \lambda_1\langle 0(\beta)|\psi_\downarrow(x,i)\psi_\uparrow(x,i)|0(\beta)\rangle \tag{2.5}$$

and

$$\Delta_2(T) = \lambda_2\langle 0(\beta)|\psi_\downarrow(x,i)\psi_\uparrow(x,i+1)|0(\beta)\rangle \tag{2.6}$$

$$= \lambda_2\langle 0(\beta)|\psi_\downarrow(x,i)\psi_\uparrow(x,i-1)|0(\beta)\rangle , \tag{2.7}$$

where the z-reflection symmetry was considered. The state vector $|0(\beta)\rangle$ is the thermal vacuum at temperature $T=1/k_B\beta$. Although here we used the notion of the thermal vacuum in the thermofield dynamics (TFD), the readers are not required to have a knowledge of TFD in order to understand this paper, they can read the thermal vacuum expectation value as the thermal average. We use the TFD notation because we plan to extend our future analysis to include the Goldstone boson current effects when we analyze magnetic properties, as we did in the previous paper with $\lambda_1=0$. In this paper we concentrate on analysis of the order parameters.

With the mean-field approximation we obtain the following gap equations:

$$\Delta_1 = A\int_0^{\omega_c} d\varepsilon \int_0^{\pi} dx \frac{\Delta_1+\Delta_2\cos x}{E}[1-2f_F(E)] , \tag{2.8}$$

$$\Delta_2 = B\int_0^{\omega_c} d\varepsilon \int_0^{\pi} dx \frac{(\Delta_1+\Delta_2\cos x)\cos x}{E}[1-2f_F(E)] . \tag{2.9}$$

Here, E is the energy of the quasielectron, $E=[\varepsilon^2+(\Delta_1+\Delta_2\cos x)^2]^{1/2}$. Other notations are $x=k_z a$, $A=(\lambda_1 m)/(2\pi^2)$, and $B=(\lambda_2 m)/(2\pi^2)$. The $f_F(E)$ is the electron distribution function,

$$f_F(E) = (1+\exp\beta E)^{-1} .$$

The cutoff energy ω_c is an unknown parameter because we do not specify the mechanism for mediating electron interactions. We used the same ω_c for the bridge and in-sheets pairs by assuming the same mechanism for creation of these pair interactions. We omit the argument T in the functions $\Delta_1(T)$ and $\Delta_2(T)$ when there is no confusion.

The tunneling interaction controls the anisotropic properties of the energy gap. The structure of the electron energy spectrum indicates that the energy gap Δ_G is given by

$$\Delta_G = \min_x\{|\Delta_1+\Delta_2\cos x|\} .$$

When $\Delta_1<\Delta_2$, this energy gap vanishes at a certain value of k_z, implying that the superconductivity is a gapless one.

Intuitively we see that the third component of the momentum k_z is created by the electron tunneling caused by the bridge pairing interaction. This can be seen from the above gap equations in which k_z appears only through the expression $\Delta_2\cos(k_z a)$. This indicates that, when Δ_2 vanishes, the k_z freedom disappears. This is important when we recall that the mean-field approximation becomes unreliable when $\Delta_2=0$ because then an infrared quantum fluctuation destroys the two-dimensional superconductivity without k_z freedom. To see how the electron tunneling removes the infrared catastrophe and stabilizes the multisheet superconductivity, we need the ap-

proximation beyond the mean-field approximation. This will be studied in Sec. IV B, where the electromagnetic effects including the Coulomb potential effects are considered.

When $A=0$ (i.e., $\lambda_1=0$), the present model reduces to the one studied in a previous paper.[11] In this case we have only the second gap equation (2.9) with $\Delta_1=0$. This gap equation was studied in a previous paper and the gap at $T=0$ was found to be

$$\Delta_2(0)=2\omega_c I \exp\left[-\frac{2}{\pi B}\right] \tag{2.10}$$

with the constant I defined by

$$I=\exp\left[-\frac{4}{\pi}\int_0^{\pi/2} dx\, \cos^2 x \ln\cos x\right] . \tag{2.11}$$

The critical temperature T_c is

$$T_c=(2\omega_c \exp[-2/\pi B])/(k_B \pi \exp[-\gamma]) . \tag{2.12}$$

When $B=0$ (i.e., $\lambda_2=0$), we have only the first gap equation (2.8) with $\Delta_2=0$. However, in this case the gap equation does not contain k_z, meaning that the electron tunneling disappears and each sheet becomes an isolated two-dimensional sheet. In this case the mean-field calculation becomes unreliable because the infrared quantum fluctuation is ignored. Thus we cannot trust the above equation when $\Delta_2=0$. We come back to this point in Sec. IV B. Although the superconductivity given by the mean-field approximation with $\lambda_2=0$ (i.e., $\Delta_2=0$) is not realistic, we denote Δ_1 given by this mean-field approximation by $\Delta_{\rm BCS}(T)$ because each isolated sheets acts as the two-dimensional BCS model. The critical temperature of this fictitious model is denoted by $T_{\rm BCS}$. We then find

$$k_B T_{\rm BCS}=[2\omega_c/\pi \exp(-\gamma)]\exp[-1/\pi A]$$

with γ being the Euler constant ($\gamma=0.577\,21$), and

$$\Delta_{\rm BCS}(0)=2\omega_c \exp[-1/\pi A] .$$

Solving the gap equations (2.8) and (2.9) is not a simple task. The numerical computations are simplified by use of the reduced parameters, such as $\Delta_i(T)/\Delta_{\rm BCS}(0)$ and $T/T_{\rm BCS}$. However, to analyze the numerical results it is convenient to scale the other parameters and the temperature in terms of $\Delta_2(0)$ and T_2. We thus define the reduced order parameters and the reduced temperature as

$$\delta_i=\frac{\Delta_i(T)}{\Delta_2(0)}, \quad i=1,2 , \tag{2.13}$$

$$t=\frac{T}{T_c} . \tag{2.14}$$

Here T_c is the critical temperature. We use $\Delta_2(0)$ for the unit of the order parameter because the superconductivity in this paper is maintained by the electron tunneling which is the origin of the bridge pair order parameter $\Delta_2(T)$. The critical temperature is given by the temperature T_2 at which $\Delta_2(T)$ vanishes. However, in the case of mean-field fictitious superconductivity of the isolated two-dimensional system mentioned above, T_c is given by $T_{\rm BCS}$.

We are going to see that the following constant c plays a key role in analysis of the multisheet model:

$$c=\frac{1}{2}+\frac{1}{\pi A}-\frac{2}{\pi B} . \tag{2.15}$$

III. ZERO TEMPERATURE

Let us first consider $T=0$. In this case we can solve the gap equations analytically in the range $0\le c\le 3/2$. We find

$$\Delta_1(0)=4\omega_c\sqrt{c}\,\exp\left[-\left[\frac{1}{\pi A}+1\right]\right] , \tag{3.1}$$

$$\Delta_2(0)=4\omega_c \exp\left[-\left[\frac{1}{\pi A}+1\right]\right] , \tag{3.2}$$

for $\Delta_1(0)<\Delta_2(0)$, while for $\Delta_1(0)>\Delta_2(0)$ we have

$$\Delta_1(0)=\frac{2}{1+D}\exp(D-1) \tag{3.3}$$

with

$$D=\left[1-\left[\frac{\Delta_2(0)}{\Delta_1(0)}\right]^2\right]^{1/2} , \tag{3.4}$$

$$=\frac{c-1}{2}+\left[\left[\frac{c-1}{2}\right]^2+c-1\right]^{1/2} . \tag{3.5}$$

Combining (3.3) and (3.4) we can write $\Delta_2(0)$ in terms of c and A.

Simple calculations lead us to

$$\Delta_1(0)<\Delta_2(0) \quad \text{for } 0<c<1 ; \tag{3.6}$$

$$\Delta_1(0)>\Delta_2(0) \quad \text{for } 1<c\le\tfrac{3}{2} , \tag{3.7}$$

$$\Delta_1(0)=\Delta_2(0) \quad \text{for } c=1 . \tag{3.8}$$

Thus, D is defined only in the range $1<c\le\frac{3}{2}$. When $c=\frac{3}{2}$, we find $D=1$, which, together with (3.4), gives $\Delta_2(0)=0$.

We now turn to the range outside of $0\le c\le\frac{3}{2}$. Here the results are obtained by a numerical computation. When $c<0$, we find $\Delta_1(0)=0$. In this case the order parameter Δ_2 is the same as the one studied in the previous paper and therefore is given by (2.10). A remarkable fact is that $c<0$ is not attained by the limit $A\to 0$. Therefore, both $c<0$ and $A=0$ gives (2.10), although the vanishing limit of A gives positive c. In this sense $A=0$ is a singular point in the domain of the parameter A. Thus, the in-sheet pairs disappear under one of two conditions: $c<0$ or $A=0$. In the previous paper we studied the latter condition.

When $c>\frac{3}{2}$ we find $\Delta_2(0)=0$, meaning no k_z freedom and therefore no tunneling. As it was pointed out, in this case the mean-field approximation is not reliable and the superconductivity is expected to be unstable.

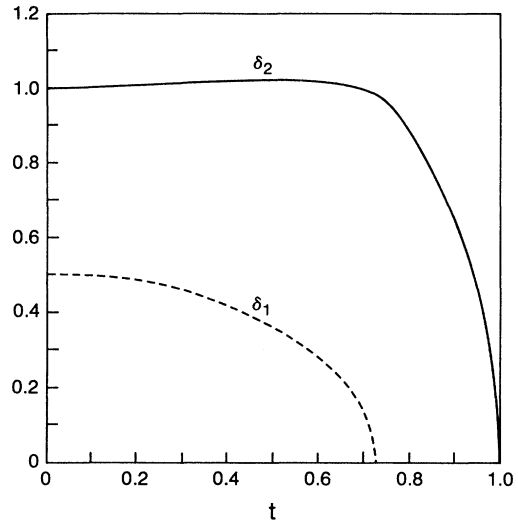

FIG. 1. $\delta_1(t)=\Delta_1(T)/\Delta_2(0)$, $\delta_2(t)=\Delta_2(T)/\Delta_2(0)$, $t=T/T_c$, $c=0.25$. Note that $\delta_2(t)$ has a kink at t_1.

The above consideration showed that the multisheet superconductivity with both the bridge and in-sheet pairs is quite different from the one without the in-sheet pair. When A becomes very small and B is fixed, we find that the bridge pair order parameter $\Delta_2(0)$ rapidly diminishes. On the other hand, the larger B (i.e. stronger bridge pair interaction) with fixed A enhances the in-sheet pair order parameter $\Delta_1(0)$, and the smaller B reduces the in-sheet pair order parameter. [An exception is $A=0$, which gives vanishing $\Delta_1(0)$ with nonvanishing $\Delta_2(0)$, which is

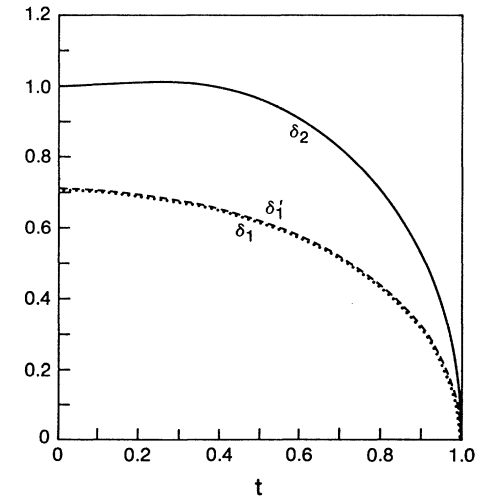

FIG. 2. $\delta_1(t)=\Delta_1(T)/\Delta_2(0)$, $\delta_1'(t)=\Delta_1'(T)/\Delta_2(0)$, $\delta_2(t)=\Delta_2(T)/\Delta_2(0)$, $t=T/T_c$, $c=0.5$. δ_1' contains the infrared effect which is not included by the mean-field approximation. This figure shows that the mean-field approximation is quite good practically everywhere in the temperature range below T_c, except at T_c where δ_1' sharply drops to zero.

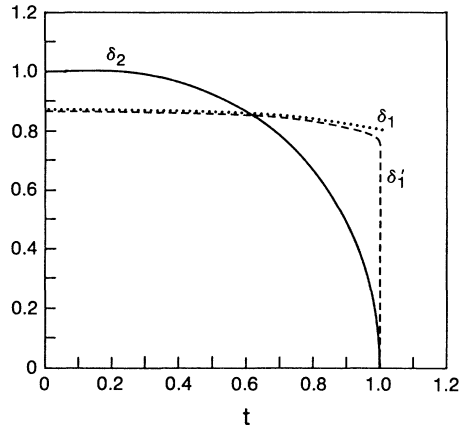

FIG. 3. $\delta_1(t)=\Delta_1(T)/\Delta_2(0)$, $\delta_1'(t)=\Delta_1'(T)/\Delta_2(0)$, $\delta_2(t)=\Delta_2(T)/\Delta_2(0)$, $t=T/T_c$, $c=0.75$.

given by (2.10).] To keep the superconducting state, the bridge pair interaction and the in-sheet one should make a reasonable balance. Considering all the possibilities including the exception mentioned above, we see that nonvanishing B is needed to maintain the superconductivity. This is intuitively reasonable because the tunneling maintains the superconductivity.

IV. FINITE TEMPERATURE

In this section we present the results for finite temperature which are obtained by a numerical computation applied to the gap equations (2.8) and (2.9). We will also briefly study the specific heat and free energy for certain values of c.

A. Mean-field approximation

Here we present the results of these gap equations without any correction. However, when $\Delta_1 \neq 0$ with

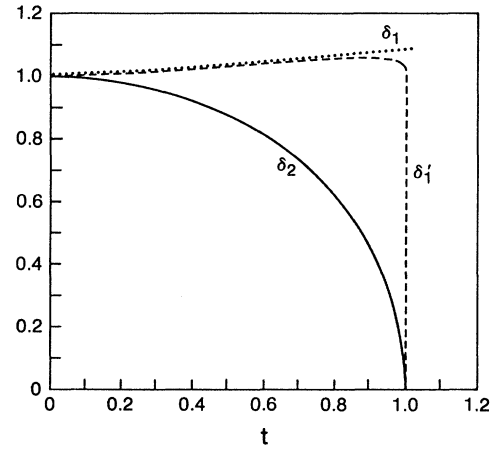

FIG. 4. $\delta_1(t)=\Delta_1(T)/\Delta_2(0)$, $\delta_1'(t)=\Delta_1'(T)/\Delta_2(0)$, $\delta_2(t)=\Delta_2(T)/\Delta_2(0)$, $t=T/T_c$, $c=1$.

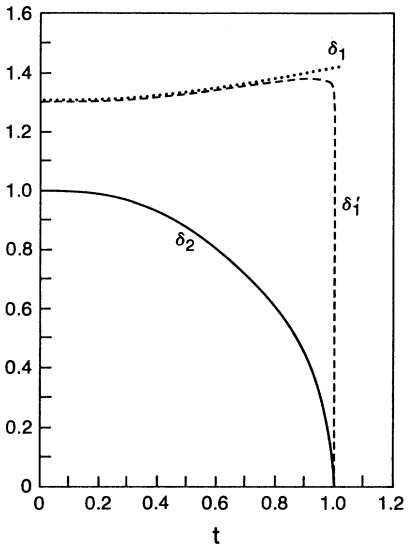

FIG. 5. $\delta_1(T)=\Delta_1(T)/\Delta_2(0)$, $\delta_1'(t)=\Delta_1'(T)/\Delta_2(0)$, $\delta_2(t)=\Delta_2(T)/\Delta_2(0)$, $t=T/T_c$, $c=1.25$.

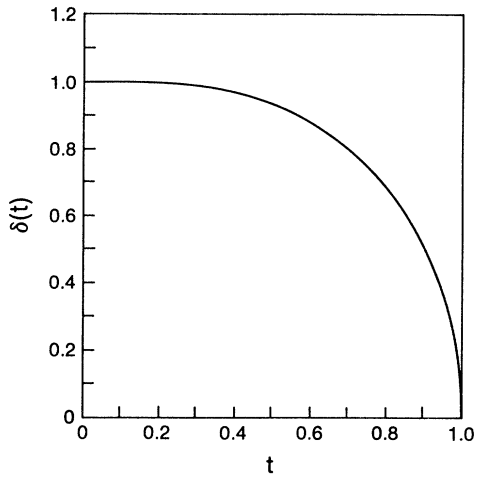

FIG. 6. $\delta(t)=\Delta_2(T)/\Delta_2(0)$, $t=T/T_c$, $\lambda_1=0$. (The model studied in Ref. 11.)

$\Delta_2=0$, the mean-field approximation is not reliable and we need to take into account the infrared fluctuation effect. This will be discussed in the next subsection.

Now we summarize the numerical solutions to the above two gap equations. The numerical results are classified by the parameter c. In Figs. 1–5, we plot $\delta_1(t)$ and $\delta_2(t)$ versus reduced temperature t with $c=0.25$, 0.5, 0.75, 1, and 1.25, respectively. In this paper the temperatures T_1 and T_2 are defined as follows: Δ_1 vanishes at $T=T_1$ and Δ_2 vanishes at $T=T_2$ with increasing temperature, respectively. Their reduced values are $t_1=T/T_1$ and $t_2=T_2/T_c$. Since T_2 is T_c we have $t_2=1$.

Figure 1 illustrates the general behavior of order parameters for $c<0.5$. There we have $\Delta_2(T)>\Delta_1(T)$ for any T and therefore the electron energy gap is zero, implying the gapless superconductivity. The critical temperature is given by $T_c=T_2$. Since $\Delta_1(T)$ is zero at T around T_c, the T_c is the same as the one for the model with $\lambda_1=0$, which was studied in a previous paper.[11] Thus, T_c is given by (2.12). In Fig. 1, t_1 is around 0.727. For the sake of comparison, we plot, in Fig. 6, $\delta(t)$, which is the bridge pair reduced order parameter $\delta_2(t)$ for the model without intrasheet interaction (i.e., $\lambda_1=0$) and was obtained in a previous paper. Since $T_2>T_1$, the infrared fluctuation is negligible and therefore the mean-field approximation is reliable. In this case, therefore, we proceed to compute the specific heat and free energy.

The specific heat is given by

$$c_s(T)=T\left[\frac{\partial s}{\partial T}\right], \tag{4.1}$$

where s is the entropy density

$$s(T)=-2a\int\frac{d^2k}{(2\pi)^2}\int_{-\pi}^{\pi/a}\frac{dk_z}{2\pi}\{f_F(E_k)\ln[f_F(E_k)]+[1-f_F(E_k)]\ln[1-f_F(E_k)]\}\ . \tag{4.2}$$

We then obtain

$$c_s(T)=-2a\int\frac{d^2k}{(2\pi)^2}\int_{-\pi/a}^{\pi/a}\frac{dk_z}{2\pi}\left[E_k^2+\frac{\beta}{2}\frac{\partial}{\partial\beta}[\Delta_1+\Delta_2\cos(k_z a)]^2\right]\frac{\partial f_F(E_k)}{\partial E_k}\ . \tag{4.3}$$

The superconducting free energy $F^s(T)$ is

$$F^s(T)=\frac{4\pi m}{(2\pi)^3}\int_0^{\omega_c}d\varepsilon\int_{-\pi}^{\pi}dx\left[-E+\frac{E^2-\varepsilon^2}{2E}[1-2f_F(E)]\right]+\frac{2}{\beta}\frac{4\pi m}{(2\pi)^3}\int_0^{\omega_c}d\varepsilon\int_{-\pi}^{\pi}dx\ln[1-f_F(E)]\ , \tag{4.4}$$

while the normal conducting free energy $F^n(T)$ is

$$F^n(T)=\frac{2}{\beta}\frac{4\pi m}{(2\pi)^3}\int_0^{\omega_c}d\varepsilon\int_{-\pi}^{\pi}dx\ln[1-f_F(E)]\ . \tag{4.5}$$

We plot the specific heat versus temperature from zero up to T_c in Fig. 7, in which we see that there is a small jump with a visible kink near t_1 caused by disappearance of δ_1. The behavior of the free energy in Fig. 8 shows that this is a second-order phase transition. Thus, in this case we may observe one jump with kink at t_1 and one

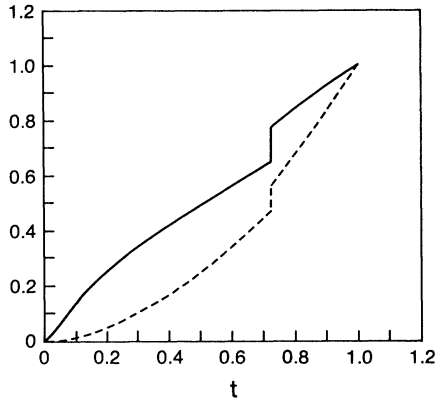

FIG. 7. The reduced specific heat $c_s(T)/c_s(T_c)$ vs the reduced temperature $t=T/T_c$ for $c=0.25$. The disappearance of $\delta_1(t)$ at t_1 creates a kink with a small jump.

peak at $t_2=1$ in the specific-heat curve. The calculation of the change of the specific heat at the critical temperature with $c=0.25$ gives

$$\frac{c_s(t=1)-c_n(t=1)}{c_n(t=1)}=0.95\ . \tag{4.6}$$

In Fig. 2 we have the case for $c=0.5$. In this case the two order parameters disappear simultaneously at the critical temperature: $t_1=t_2=1$. Therefore, the specific heat exhibits only one peak.

For $c>0.5$ we find that $T_2<T_1$, implying that δ_1 remains not vanishing in the temperature range $T_1>T>T_2$, where δ_2 vanishes and therefore the tunneling disappears. Since there is no tunneling and each sheet becomes an isolated two-dimensional sheet, the superconductivity is unstable, although the mean-field approximation gives the fictitious two-dimensional BCS superconducting system with the reduced order parameter $\delta_{\rm BCS}$. In this case we should go beyond the mean-field calculation by considering the infrared effect of the collective mode. This will be discussed in the next subsection. The reduced order parameter with infrared correction will be denoted by δ_1'. We will find that δ_1' indeed vanishes at T_2. Therefore, T_2 becomes T_c (i.e., $t_2=1$) as it should do. The $T_2/T_{\rm BCS}$ is obtained from

$$1+2\int_0^\infty d\varepsilon\frac{\partial}{\partial E}f_F^{(2)}(E)=c-\tfrac{1}{2}\ , \tag{4.7}$$

which follows from the gap equations (2.8) and (2.9) with the limit $\Delta_2\to 0$. In the above equation (4.7), the notations are $E=(\varepsilon^2+\Delta_1^2)^{1/2}$ and

$$f_F^{(2)}(E)=[1+\exp(T_2E)]\ .$$

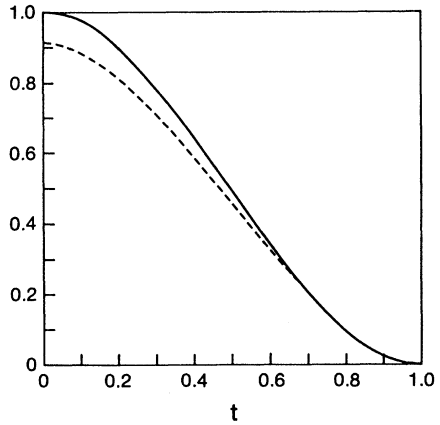

FIG. 8. The reduced free-energy difference $[F^n(T)-F^s(T)]/[(1/8\pi)H_c^2(0)]$ vs the reduced temperature $t=T/T_c$ for $c=0.25$. Here use was made of the notation $(1/8\pi)H_c^2(0)=[F^n(t=0)-F^s(\Delta_1=0,t=0)]$.

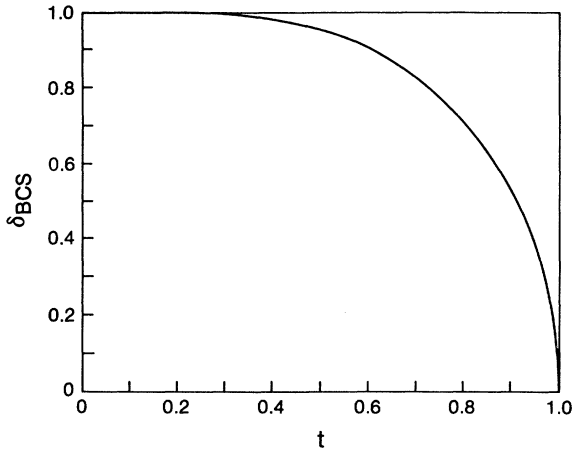

FIG. 9. The reduced two-dimensional BCS order parameter $\delta_{\rm BCS}(t)=\Delta_{\rm BCS}(T)/\Delta_{\rm BCS}(0)$ vs the reduced temperature $t=T/T_{\rm BCS}$ with the mean-field approximation.

The order parameters $\delta_1(t)$ and $\delta_2(t)$ versus t for $c=0.75$, 1, and 1.25 are presented in Figs. 3–5, respectively. For the sake of comparison we present in Fig. 9 the temperature behavior of $\Delta_{\rm BCS}$ for the fictitious two-dimensional superconductivity in the mean-field approximation.

B. Corrected order parameter

We saw in the last subsection that the mean-field approximation is not usable when $c>0.5$. To calculate the infrared correlation effect, we recall an argument which shows why the superconductivity in a two-dimensional system is unstable (see, for example, p. 308 in Ref. 6). As is well known, the superconductivity is a state of electric phase order, meaning that the electric phase symmetry is spontaneously broken.[13] Thus, there appears the Goldstone boson field χ which has no energy gap and which controls the electric phase transformation. Denoting the electron Heisenberg field operators by $\psi_\sigma(x,i)$ with σ be-

ing the spin suffix, its phase transformation $\psi_\sigma \to \exp i\theta \psi_\sigma$ is generated by the translation of the Goldstone boson, $\chi \to \chi + c$-number, with the c number being proportional to the phase θ. However, it is due to the presence of the electromagnetic field that the Goldstone field does not show up in any observable. To understand these statements, we should recall that the form of action of any operator in quantum field theory is determined when it is explicitly expressed in terms of normal products consisting of quasiparticle fields because the coefficients of the normal products are the matrix elements. In the case of superconductivity, the quasiparticles are the quasielectrons ϕ_σ, the Goldstone boson χ, and electromagnetic fields A. As it was pointed out above, in any observable, the Goldstone field χ becomes the longitudinal part of the electromagnetic field, meaning that it appears only through the combination $A - \partial\chi$ in any gauge-invariant operators. However, χ can appear independently of the electromagnetic field when it appears in an operator which is not gauge invariant. This can be seen, for example, from the structure of ψ_σ. The above argument on the phase transformation and the Goldstone theorem indicates that χ acts as the phase of ψ_σ. Thus, the expression of the electron Heisenberg field in terms of quasiparticle field takes the form

$$\psi_\sigma = :\exp\left[i\frac{Z^{1/2}}{2v}\chi\right]F_\sigma[\phi, A-\partial\chi]: . \tag{4.8}$$

Here Z is the residue of the Goldstone boson Green's function[11] $v=(2\Delta_2/\lambda_2)$ and the colons are the normal product symbol commonly used. As it will be shown in the Appendix, we have

$$Z=(32\pi/m)[\Delta_2(T)/\lambda_2]^2 ,$$

which gives $Z/(2v)^2=2\pi/m$.

The field equation of the Goldstone boson is

$$\left[\frac{\partial^2}{\partial t^2}+\omega_B^2(-i\nabla)\right]\chi(x,t) + \omega_{\rm pl}^2(-i\nabla)\int d^3y \frac{1}{4\pi|\mathbf{x}-\mathbf{y}|}\nabla^2\chi(y,t)=0 . \tag{4.9}$$

The last term is the Coulomb potential effect, $\omega_{\rm pl}$ is the plasmon energy in Fourier form, and ω_B is the Goldstone boson energy without the Coulomb potential effect. Thus, $\omega_B(0)=0$. It is due to the long-range nature of the Coulomb potential that we need a particular care in calculating the integration in the last term. If we would perform the integration in parts and would ignore the surface effect, the formula

$$\nabla^2\frac{1}{4\pi|\mathbf{x}-\mathbf{y}|}=-\delta(\mathbf{x}-\mathbf{y}) \tag{4.10}$$

would lead to the plasmon equation

$$\left[\frac{\partial^2}{\partial t^2}+\omega_B^2(-i\nabla)+\omega_{\rm pl}^2(-i\nabla)\right]\chi(x,t)=0 . \tag{4.11}$$

However, we cannot ignore the surface term because the Coulomb potential has long range. To understand a nature of the surface term we may operate both sides of Eq. (4.9) with ∇^2. The result is

$$\left[\frac{\partial^2}{\partial t^2}+\omega_B^2(-i\nabla)+\omega_{\rm pl}^2(-i\nabla)\right]\nabla^2\chi(x,t)=0 , \tag{4.12}$$

which shows that χ, with nonvanishing momentum, becomes a plasmon. This situation has sometimes been briefly described by the statement that the Coulomb interaction changes the Goldstone boson of almost an entire momentum domain, except infinitesimal momentum, into the plasmon. This is called the Anderson-Higgs-Kibble mechanism. The presence of the Goldstone mode with infinitesimal momentum is significant in many ways. First, the above-mentioned transformation $\chi \to \chi + c$-number is only induced by the zero-momentum part of the Goldstone boson. Second, this infrared part of the Goldstone mode is the origin of the vortices. A careful treatment of Eq. (4.9) is to put it in the Fourier form and to introduce the low-momentum cutoff η in the integration with the Coulomb potential. This leads to the plasmon equation (4.11) for $|\mathbf{k}|>\eta$, while we still have the Goldstone equation

$$\left[\frac{\partial^2}{\partial t^2}+\omega_B^2(-i\nabla)\right]\chi(x,t)=0 \quad \text{for } |\mathbf{k}|<\eta . \tag{4.13}$$

We perform the limit $\eta \to 0$ at the end of the entire calculation. In the case under consideration, we perform this limit only after we finish calculation of the order parameters. We will then find that the corrected order parameter vanishes as soon as the bridge pair order parameter disappears. This calculation will be presented in the following.

In the mean-field approximation we regard ψ as ϕ in the calculation of order parameters. To improve this, we put

$$\psi = \exp[i(Z^{1/2}/2v)\chi]\phi .$$

Then the corrected order parameter Δ_1' for the in-sheet pair becomes

$$\Delta_1' = \Delta_1 \exp\left[-\frac{1}{2}\frac{Z}{(2v)^2}D(0)\right] . \tag{4.14}$$

Here $D(0)$ is

$$D(0)=\langle 0(\beta)|\chi(x_1,i)\chi(x_2,j)|0(\beta)\rangle \tag{4.15}$$

with $x_1=x_2$ and $i=j$. We easily obtain

$$D(0)=\frac{a}{2(2\pi)^2}\int_0^\eta dk \int_{-\pi/a}^{\pi/a} dk_z \frac{k}{\omega(k,k_z)} \times \frac{1}{\exp[\beta\omega(k,k_z)]-1} , \tag{4.16}$$

where η is a cutoff momentum and $\omega(k,k_z)$ is the Goldstone energy, which was calculated in a previous paper[11] as

$$\omega^2(k,k_z)=\tfrac{1}{2}v_F^2k^2+\tfrac{1}{2}(a\Delta_2)^2k_z^2 \ . \tag{4.17}$$

Here v_F is the Fermi velocity. To analyze the infrared effect we use a small η so that $[\exp(\beta\omega)-1]$ is approximately replaced by $\beta\omega$. We then obtain

$$D(0)=\frac{a}{2(2\pi)^2\beta}\int_0^{\eta}dk\int_{-\pi/a}^{\pi/a}dk_z\frac{k}{[\omega(k,k_z)]^2} \ . \tag{4.18}$$

When $\Delta_2=0$, this diverges, leading to the vanishing Δ_1' according to (4.14). This shows how the superconductivity becomes unstable when the tunneling disappears. With (4.14) we can calculate the corrected order parameter. When Δ_2 is small, $D(0)$ becomes $(1/4\pi\beta v_F^2)\ln[\Delta_2]^2$. We thus have

$$\Delta_1'(T)=[\Delta_2(T)]^{\frac{1}{2}\beta m v_F^2}\Delta_1(T) \ . \tag{4.19}$$

Note that the correction factor is unity at $T=0$, as it should be. Further consistency can be seen in the fact that $\Delta_1'=0$ when $\Delta_2=0$.

When we take $T_c=100$ K and $v_F=10^5$ m/s, we have

$$\delta_1'(t)=\left[\frac{\delta_2(t)}{\delta_2(0)}\right]^{0.08T/T_c}\delta_1(t) \tag{4.20}$$

for the corrected reduced order parameter. In Figs. 3–5 we plot $\delta_1(t)$, $\delta_2(t)$, and $\delta_1'(t)$ for $c=0$, 75, 1, and 1.25, respectively. In these figures, we see that the mean-field approximation is quite good unless the temperature is extremely close to the critical temperature. In all these cases, δ_1' drops sharply around the critical temperature. This is a possible explanation for the observed anomalous behavior of specific heat near the critical temperature.[14] The computation of specific heat and free energy for $c>0.5$ is underway.

It is interesting to study the energy gap

$$\Delta_G=\min|\Delta_1'+\Delta_2\cos k_z a|$$

for these cases. We plot Δ_G in Fig. 10. We see that, in a certain range of temperature, the energy gap increases with increasing temperature. The superconductor remains gapless with increasing temperature, especially when $c=0.75$, until a certain temperature is reached. The energy gap drops to zero rapidly when the temperature approaches the critical temperature.

We have seen several features of multisheet superconducting system. The behavior depends on the materials through the parameter c.

V. A SHORT SUMMARY

In this paper we have studied the behavior of order parameters in a multisheet superconducting system with intersheet and intrasheet interactions. The results are consistent with the following physical picture. In a system with both intersheet and intrasheet interactions, there can be two kinds of Cooper pairs: one is the bridge pair and another is the in-sheet pair. The superconducting system is maintained by the bridge pairs. When the bridge pair breaks, the tunneling disappears and, as a result, the in-sheet pair also breaks due to the infrared effect of the collective mode. The main properties of superconductivity are mostly controlled by the characteristic parameter c which consists of the intersheet and intrasheet couplings. With different c, different samples exhibit different behavior. We saw that a too-weak in-sheet pair interaction with a finite bridge pair interaction will destroy bridge pairs instead of in-sheet pairs. Likewise, in order to have an in-sheet pair superconductor, the bridge pair interaction should not be too small. We find that, in materials with $0<c<0.5$, one peak and one jump appear with a kink in the specific heat. To analyze the specific heat of materials with $0.5<c<1.5$, we should improve the approximation beyond the mean-field approximation by considering the infrared effect discussed in Sec. IV B. This analysis is in progress. In our next paper we will extend our analysis to also include the magnetic properties of mixed states.

We close this summary with an interesting feature particular to systems of low-dimensional structure. Recall the bridge pairs studied in this paper. In the bridge pairs each electron belongs to two pairs, forming a chain of pairs. We say that the pair multiplicity is two (see Fig. 11). The wave function of chained pairs may exhibit a strong correlation. It is intuitively expected that a higher multiplicity may make a tighter correlation. This argument suggests that to increase the pair multiplicity may be one way to make a strong correlation. To see how the

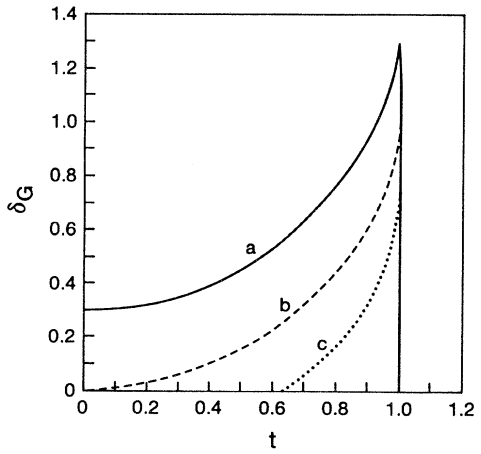

FIG. 10. The reduced energy gaps $\delta_G=\Delta_G/\Delta_{\rm BCS}(0)$ vs $t=T/T_{\rm BCS}$ for $c=0.75$, 1, 1.25 are presented.

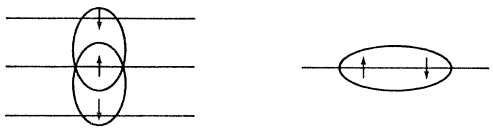

FIG. 11. The bridge pairs in a multisheet system are illustrated. The pair multiplicity of the bridge pairs is 2 while that of the in-sheet pairs is 1.

pair multiplicity is related to the dimension, let us suppose a system of lines with such a structure that each line is surrounded by n lines. When the electrons in the nearest lines form Cooper pairs, we can have pairs with multiplicity n. In this way we see that the lower dimension can accommodate higher multiplicity of pairs, thus enhancing correlations. This aspect of the low dimensionality may compete with the destructive aspect due to the fluctuation effect enhanced by the low dimensionality. This competition may open an intricate behavior of long-range correlations in a system of low dimension. The study of pair multiplicity in organic superconductors poses a particularly interesting research problem. We plan to make a systematic study of pair multiplicity effects.

ACKNOWLEDGMENTS

We would like to thank Dr. J. Whitehead for useful discussion. One of us (Z. Ye) would like to thank Sanjay Chugh for constant encouragement and discussion. This work was supported by Natural Sciences and Engineering Research Council (NSERC), Canada and the Dean of Science, the University of Alberta.

APPENDIX

In Sec. IV B we calculated the correction in the order parameter Δ_1. The correction was due to the infrared effect of the Goldstone boson. In this calculation there appeared the constant Z, which is the residue of the Green's function of the Goldstone boson. Here we present the calculation of factor Z. According to a previous paper,[11] we have, for small k,

$$Z=\frac{2}{\lambda_2 R_{0,\beta}}\ , \tag{A1}$$

where $R_{0,\beta}=R_{\|,\beta}/2\Delta^2$ with $R_{\|,\beta}$ being given by

$$R_{\|,\beta}=(\lambda_2 m)\int_0^{\omega_c}\frac{d\varepsilon}{\pi}\int_{-\pi}^{\pi}\frac{dx}{2\pi}\left[\frac{1}{2E^3}\{\cos^2x\,(E^2+\varepsilon^2)-\varepsilon^2+\tfrac{1}{2}\Delta_2^2\cos^2x\,[1-f_F(E)]\}\right.$$
$$\left.+\frac{1}{E^3}\Delta_2^2\cos^2x(\cos^2x-\tfrac{3}{2})\beta f_F(E)[1-f_F(E)]\right]\ . \tag{A2}$$

Since $R_{\|,\beta}$ depends mildly on temperature, we approximately calculate it at zero temperature. Then a simple calculation leads to

$$R_{\|,\beta}=\frac{\lambda_2 m}{8\pi}\ , \tag{A3}$$

which gives

$$R_{0,\beta}=\frac{\lambda_2 m}{16\Delta_2^2\pi}\ . \tag{A4}$$

Thus, we have

$$Z(0)=\frac{32\pi}{m}\left[\frac{\Delta_2}{\lambda_2}\right]^2\ . \tag{A5}$$

[1]S. W. Cheong, J. D. Thompson, and Z. Fisk, Physica C **158**, 109 (1989).
[2]A. G. Klimenko, Phys. Lett. A **138**, 439 (1989).
[3]R. R. Gerhardts, Phys. Rev. B **9**, 2945 (1974).
[4]Z. Gulacsi, M. Gulacsi, and I. Pop, Phys. Rev. B **37**, 2247 (1988).
[5]T. Rice, Z. Phys. B **67**, 141 (1987).
[6]H. Umezawa, H. Matsumoto, and M. Tachiki, *Thermo Field Dynamics and Condensed States* (North-Holland, Amsterdam, 1982).
[7]T. Koyama, N. Takezawa, and M. Tachiki, Physica C **168**, 69 (1990).
[8]J. P. Strobel, A. Thoma, B. Hensel, H. Adrian, and G. Saeman-Ischenco, Physica C **153-155**, 1537 (1988).
[9]A. Umezawa, G. W. Crabtree, K. G. Vandervoort, U. Welp, W. K. Kwok, and J. Z. Liu, Physica C **162-164**, 329 (1989).
[10]H. Safar, H. Pastoriza, D. J. Bishop, L. F. Schneemeyer, and J. V. Waszczak, Phys. Rev. B **43**, 13 610 (1991).
[11]Z. Ye, H. Umezawa, and R. Teshima, Solid State Commun. **74**, 1327 (1990).
[12]T. Schneider, H. De Raedt, and M. Frick, Z. Phys. B **76**, 3 (1989).
[13]L. Leplae, H. Umezawa, and F. Mancini, Phys. Rep. C **10**, 153 (1974).
[14]E. Braun, W. Schnelle, F. Seidler, P. Böhm, W. Brauwish, Z. Drzazga, S. Ruppel, H. Broicher, H. Geus, M. Galffy, B. Roden, I. Felner, and D. Wohlleben, Physica C **162-164**, 496 (1989).